Mathematical Modeling and Simulation of Flying Robots

Micael S. Couceiro [1], *N. M. Fonseca Ferreira* [2], *Rui Rocha* [1]

[1] Institute of Systems and Robotics, University of Coimbra,
Pólo II, 3030-290 Coimbra, Portugal
{micaelcouceiro, rprocha}@isr.uc.pt

[2] Department of Electrical Engineering, Institute of Engineering of Coimbra
Rua Pedro Nunes, 3031-601 Coimbra, Portugal
nunomig@isec.pt

Abstract: This paper covers a wide knowledge of dynamical flying models. Firstly, we provide an overview of the different implemented models. Secondly, we provide the simulation platforms of the implemented models.
The objective of this work is to develop simulation environments implementing the mathematical modeling of several different flying platforms using the high-level calculation tool *MatLab* and the modeling, simulation and analysis of dynamic systems tool *Simulink*.

Keywords: simulation, modeling, flying.

1. INTRODUCTION

In this study we consider the mathematical modeling and control of a variety of systems with different characteristics (e.g., degrees of freedom, flying methods and others). We will mainly focuses in flying robots similar to helicopters such as the *TRMS* - Twin Rotor MIMO System – [1], the Quad-Rotor [2] and the real helicopter [3].

Engineers have long been stymied in their attempts to fabricate flying robots that can match the amazing flight capabilities of nature's most advanced flying creatures. Such robot could be used for a variety of tasks, from spying, to mine detection to search and rescue missions in collapsed buildings [4] [5]. The study of dynamic models based on birds and insects has been extended and shows some results that can be considered very close to the real model [6], [7] and [8]. In the last few years, there were significant advances in robotics, artificial intelligence and other fields allowing the implementation of biologically inspired robots [9] [10].

The paper is organized as follows. Section two develops the mathematical model of each different platform describing the *TRMS*, the Quad-Rotor and the real helicopter dynamics implemented. Section three shows a general overview of a variety of the implemented simulators and describes its main features and commands of each simulator. Finally, outlines the main conclusions in section four.

2. HELICOPTER MODELS

Historical flight documents have hundreds of failed helicopter projects [11]. Most of them were made based on hope in flying at any cost. However, some of these designs provided a significant contribution to a new understanding that ultimately led to the successful improvement of the modern helicopter. Yet, it was not until the more technical contributions of engineers such as Juan de la Cierva, Henrich Focke, Raoul Hafner, Harold Pitcairn, Igor Sikorsky, Arthur Young, and others, that the design of a truly safe and practical helicopter becomes a reality [12].

In order to establish a methodology and appropriated strategy to this project, it is important to study the aerodynamic principles knowing that those will be crucial to the physics behind the flight of birds.

Several studies in this area have been made and are focusing on the mathematical modeling of both linear and nonlinear dynamics [8]. The analysis of dynamical linear models is well established in the current literature [13] [14].

The dynamics of flight is concerned with the overall dynamic behavior of an aircraft: stability, controllability, the dynamic response, the quality control, etc. However the analysis of flight dynamics requires a simple and effective model. This model should be valid for all combinations of angle-of-attack, gravitational acceleration, speed and altitude reached in which the model operates.

2.1. TRMS – Twin Rotor MIMO System

The study concerning the ability to control helicopters was improved with the Twin Rotor MIMO System – *TRMS* (Fig. 1). It consists on a laboratory set-up designed for control experiments. In certain aspects its behavior resembles that of a helicopter. From the control point of view it exemplifies a high order nonlinear system with significant cross-couplings. A mathematical model design of *TRMS* needs knowledge of aero dynamical physic laws.

Fig. 1. Laboratory platform TRMS.

The *TRMS* (Fig. 2) has two *dof*, namely, the rotation of the helicopter body with respect to the horizontal axis and the rotation around the vertical axis. Each axis has one potentiometer for measuring the correspondent angle. The helicopter can move in the range -170º < a_h < 170º, and -60º < a_v < 60º, around the horizontal and vertical axis, respectively. The inputs of the model are the motor voltages U_h and U_v affecting the main and tail rotors. The output command must match the capabilities of the hardware board that is capable to outputing a [0, 5] Volt signal. This signal is shifted in the amplifier to create ±2.5 Volt capability required to command the drive motor in both directions. When no control signals are applied, the helicopter will tend to position at a_h = -60º.

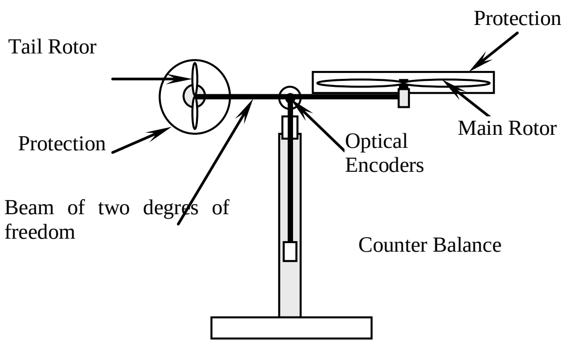

Fig. 2. TRMS model.

The physical model is developed under some simplifying assumptions [15]. It is assumed that friction is of viscous type and that the propeller air subsystem can be described in accordance with the postulates of flow theory.

First, we consider the rotation of the beam in the vertical plane, around the horizontal axis. Having in mind that driving torques are produced by the propellers, the rotation can be described by the pendulum motion principle. From the Newton second law of motion we obtain:

$$M_v = J_v \frac{d^2\alpha_v}{dt^2} \tag{1}$$

where M_v is the total moment of forces in the vertical plane, J_v is the sum of moments of inertia to the horizontal axis α_v is the pitch angle of the beam and:

$$M_v = \sum_{i=1}^{4} M_{vi} \tag{2a}$$

$$J_v = \sum_{i=1}^{8} J_{vi} \tag{2b}$$

To determine the moments of gravity forces applied to the beam, making it rotate around the horizontal axis, we consider the situation in Fig. 5, and:

$$M_{v1} = g[A - B]\cos\alpha_v - C\sin\alpha_v \tag{3a}$$

$$A = \left(\frac{m_t}{2} + m_{tr} + m_{ts}\right) l_t \tag{3b}$$

$$B = \left(\frac{m_m}{2} + m_{mr} + m_{ms}\right) l_m \tag{3c}$$

$$C = \frac{m_b}{2} l_b + m_{cb} l_{cb} \tag{3d}$$

where M_{v1} is the return torque corresponding to the forces of gravity, m_{mr} is the mass of the main DC-motor with main rotor, m_m is the mass of main part of the beam, m_{tr} is the mass of the tail motor with tail rotor, m_t is the mass of the tail part of the beam, m_{cb} is the mass of the counter-weight, m_b is the mass, of the counter-weight beam, m_{ms} is the mass of the main shield, m_{ts} is the mass of the tail shield, l_m is the length of main part of the beam, l_t is the length of tail part of the beam, l_b is the length of the counter-weight beam, l_{cb} is the distance between the counter-weight and the joint and g is the gravitational acceleration. Also:

$$M_{v2} = l_m F_v(\omega_m) \tag{4}$$

where M_{v2} is the moment of the propulsive force produced by the main rotor, w_m is angular velocity of the main rotor and $F_v(w_m)$ denotes the dependence of the propulsive force on the angular velocity of the rotor.

$$M_{v3} = -\Omega_h^2 (A + B + C)\sin\alpha_v \cos\alpha_v \tag{5}$$

where M_{v3} is the moment of centrifugal forces corresponding to the motion of the beam around the vertical axis, and:

$$\Omega_h = \frac{d\alpha_h}{dt} \tag{6}$$

where Ω_h is the angular velocity of the beam around the vertical axis and is the azimuth angle of the beam.

To determine the moments of propulsive forces applied to the beam consider the situation given in Fig. 3.

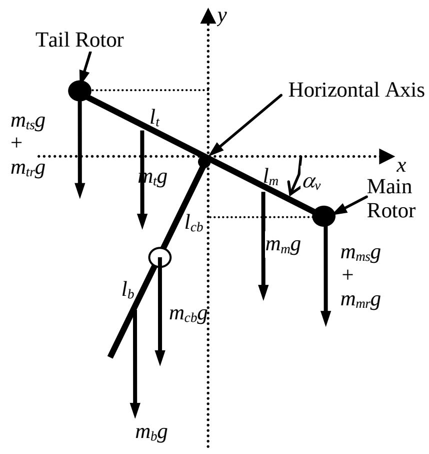

Fig. 3. Gravity forces in the TRMS, corresponding to the return torque, which determines the equilibrium position of the system.

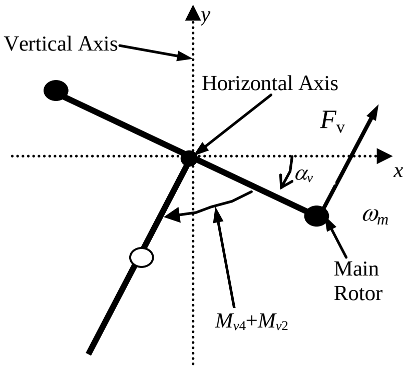

Fig. 4. Propulsive force moment and friction moment in the TRMS.

$$M_{v4} = -\Omega_v K_v \tag{7}$$

where M_{v4} is the moment of friction depending on the angular velocity of the beam around the horizontal axis, and:

$$\Omega_v = \frac{d\alpha_{vh}}{dt} \tag{8}$$

where Ω_v is the angular velocity around the horizontal axis and K_v is a constant.

According to Fig. 5 we can determine components of the moment of inertia relative to the horizontal axis. Notice, that this moment is independent of the position of the beam.

$$J_{v1} = m_{mr} l_m^2 \tag{9a}$$

$$J_{v2} = m_m \frac{l_m^2}{3} \tag{9b}$$

$$J_{v3} = m_{cb} l_{cb}^2 \tag{9c}$$

$$J_{v4} = m_b \frac{l_b^2}{3} \tag{9d}$$

$$J_{v5} = m_{tr} l_t^2 \tag{9e}$$

$$J_{v6} = m_t \frac{l_t^2}{3} \tag{9f}$$

$$J_{v7} = \frac{m_{ms}}{2} r_{ms}^2 + m_{ms} l_m^2 \tag{9g}$$

$$J_{v8} = m_{ts} r_{ts}^2 + m_{ts} l_t^2 \tag{9h}$$

where r_{ms} is the radius of the main shield and r_{ts} is the radius of the tail shield.

Similarly, we can describe the motion of the beam around the vertical axis, having in mind that the driving torques are produced by the rotors and that the moment of inertia depends on the pitch angle of the beam. The horizontal motion of the beam (around the vertical axis) can be described as a rotational motion of a solid mass:

$$M_h = J_h \frac{d^2\alpha_h}{dt^2} \tag{10}$$

where, M_h is the sum of moments of forces acting in the horizontal plane, and J_h is the sum of moments of inertia relative to the vertical axis. Then:

$$M_h = \sum_{i=1}^{2} M_{hi} \tag{11}$$

$$J_h = \sum_{i=1}^{8} J_{hi} \tag{12}$$

To determine the moments of forces applied to the beam and making it rotate around the vertical axis, consider the situation shown in Fig. 8.

$$M_{h1} = l_t . F_h(w_t) \cos\alpha_v \tag{13}$$

where w_t is the rotational velocity of tail rotor, $F_h(w_t)$ denotes the dependence of propulsive force on the angular velocity of the tail rotor which should be determined experimentally, and:

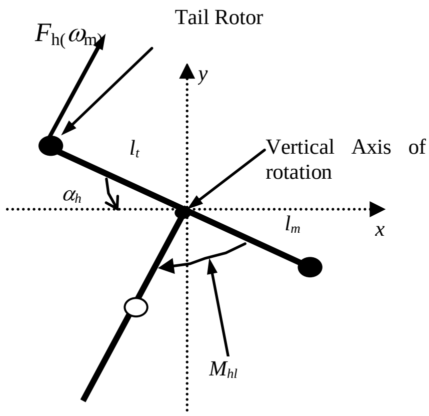

Fig. 5. Moments of forces in horizontal plane.

$$M_{h2} = -\Omega_h K_h \tag{14}$$

$$J_h = D\cos^2\alpha_v + E\sin^2\alpha_v + F \tag{16}$$

$$D = \frac{m_b}{3} l_b^2 + m_{cb} l_{cb}^2 \tag{17}$$

$$E = \left(\frac{m_m}{3} + m_{mr} + m_{ms}\right) l_m^2 + \left(\frac{m_t}{3} + m_{tr} + m_{ts}\right) l_t^2 \tag{18}$$

$$F = m_{ms} r_{ms}^2 + \frac{m_{ts}}{2} r_{ts}^2 \tag{19}$$

The helicopter motion can be describe by the equations:

$$\frac{dS_v}{dt} = \frac{l_m F_v(\omega_m) - \Omega_v K_v + G - H}{J_v} \tag{20}$$

$$G = g\left[(A-B)\cos\alpha - C\sin\alpha_v\right] \tag{21}$$

$$H = \frac{1}{2}\Omega_h^2 (A+B+C)\sin 2\alpha_v \tag{22}$$

$$\frac{d\alpha_v}{dt} = \Omega_v \tag{23}$$

$$\Omega_v = \frac{S_v + J_{tr}\omega_t}{J_v} \tag{24}$$

$$\frac{dS_h}{dt} = \frac{l_t F_h(\omega_t)\cos\alpha_v - \Omega_h K_h}{J_h} \tag{25}$$

$$\Omega_h = \frac{d\alpha_h}{dt} \tag{26}$$

$$\Omega_h = S_h + \frac{J_{tmr}\omega_m \cos\alpha_v}{J_h} \tag{27}$$

where J_{tr} is the moment of inertia in DC motor tail, J_{mr} is the moment of inertia in DV motor main, S_v is the angular momentum in vertical plane of the beam and S_h is the angular momentum in horizontal plane of the beam.

The angular velocities are a function of the DC motors, yielding:

$$\frac{du_{vv}}{dt} = \frac{1}{T_{mr}}\left(-u_{vv} + u_v\right) \tag{28}$$

$$\omega_m = P_v(u_{vv}) \tag{29}$$

$$\frac{du_{hh}}{dt} = \frac{1}{T_{tr}}\left(-u_{hh} + u_h\right) \tag{30}$$

$$\omega_t = P_h(u_{hh}) \tag{31}$$

where T_{mr} is the time constant of the main motor and T_{tr} is the time constant of the tail motor.

Finally, the mathematical model becomes a set of six non-linear equations, namely:

$$\mathbf{U} = \left[U_h \; U_v\right]^T \tag{32}$$

$$\mathbf{X} = \left[S_h \; \alpha_h \; u_{hh} \; S_v \; \alpha_v \; u_{vv}\right]^T \tag{33}$$

$$\mathbf{Y} = \left[\Omega_h \; \alpha_h \; \omega_t \; \Omega_v \; \alpha_v \; \omega_m\right]^T \tag{34}$$

where **U** is the input, **X** is the state and **Y** is the output vector.

2.2. Quad-Rotor

In 1921, a different helicopter model had appeared. De Bothezat built the first Quad-Rotor – a helicopter with 4 rotors. This model is controlled by varying the speed of each rotor, thus altering the various lift forces.

One of the advantages of using a multi-rotor helicopter is its large capacity. It has more lift capacity so larger loads can be transported. They are highly maneuverable, which allows vertical takeoff and landing, as well as the flight in areas difficult to reach. The disadvantage is the energy consumption increased due to the number of rotors. Fig. 6 shows some Quad-Rotor models.

Fig. 6. Quad-Rotor models.

Unlike conventional helicopters, the quad-rotor has fixed angles. The basic movements of this can be described using the Fig. 7.

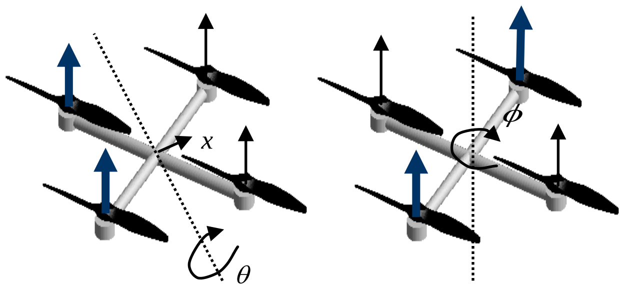

Fig. 7. Forces resulting from the movement in the *x*-axis around *z*-axis.

Is dynamically sub-acted where there are 4 control inputs and 6 output coordinates, *i.e.*, 6 degrees of freedom. The vertical motion can be obtained by equally varying the speeds of the 4 rotors at the same time. The movement along the *x*-axis is related to the inclination of the rotor *y*-axis. This approach can be obtained by increasing and decreasing the speed of rotation of the rotors 1 and 2 and increasing the speed of the rotors 3 and 4. This approach also produces motion along the *x*-axis. Similarly, the movement in the *y*-axis results of the inclination of the *x*-axis. Movements around the *z*-axis are obtained by the moments created by the rotation of the rotors. The conventional helicopters have a tail rotor in order to counter balance the moment created by the main rotor. If there are 4 rotors, the direction of rotation of each rotor is configured so that the moments cancel each other. This is also used to produce the desired rotation around *z*-axis. To rotate in clockwise direction, the speeds of the rotors 2 and 4 are scaled up to overcome the moments created by the rotors 3 and 4.

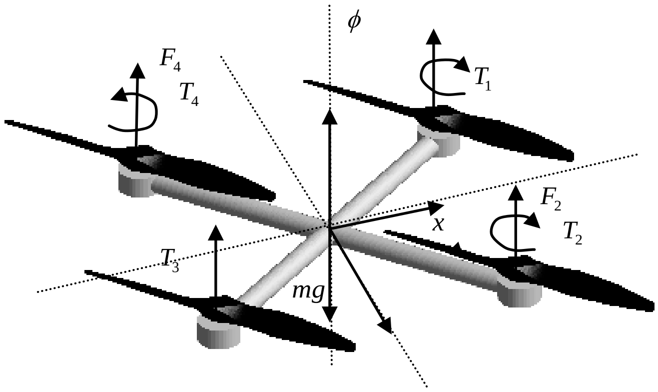

Fig. 8. Quad-Rotor model.

It is assumed that the reference of the quad-rotor is placed in the center of gravity. The axes of the quad-rotor are related to the inertial frame by vector (x, y, z) and 3 Euler angles (θ, ψ, ϕ), being θ the angle between the x-axis and the horizontal plane, ψ the angle between the y-axis and the horizontal plane and ϕ is the angle of rotation around the z-axis.

The equations of motion can be written using the balance between the forces and the moments:

$$\ddot{x} = \frac{(\sum_{i=1}^{4} F_i)(\cos\phi\sin\theta\cos\psi + \sin\phi\sin\psi) - K_1\dot{x}}{m} \quad 35a$$

$$\ddot{y} = \frac{(\sum_{i=1}^{4} F_i)(\sin\phi\sin\theta\cos\psi + \cos\phi\sin\psi) - K_2\dot{y}}{m} \quad 35b$$

$$\ddot{z} = \frac{(\sum_{i=1}^{4} F_i)(\cos\phi\cos\psi) - mg - K_3\dot{z}}{m} \quad 35c$$

$$\ddot{\theta} = l(-F_1 - F_2 + F_3 + F_4 - K_4\dot{\theta})/J_1 \quad 36a$$

$$\ddot{\psi} = l(-F_1 + F_2 + F_3 - F_4 - K_5\dot{\psi})/J_2 \quad 36b$$

$$\ddot{\phi} = l(-M_1 + M_2 + M_3 - M_4 - K_6\dot{\phi})/J_3 \quad 36c$$

where $K_i = 1, \dots, 6$ are the aerodynamic drag coefficients.

Assuming that the aerodynamic drag coefficients are negligible for low speeds, and for convenience, we define the following entries.

$$u_1 = (F_1 + F_2 + F_3 + F_4)/m \quad 37a$$

$$u_2 = (-F_1 - F_2 + F_3 + F_4)/J_1 \quad 37b$$

$$u_3 = (-F_1 + F_2 + F_3 - F_4)/J_2 \quad 37c$$

$$u_4 = C(F_1 - F_2 + F_3 - F_4)/J_3 \quad 37d$$

where $J1$, $J2$ and $J3$ are the moments of inertia in x, y, and the quad-rotor body respectively. The moments of inertia were obtained by modeling the central "hub" as a cub, the motors as cylinders, and the propellers as rigid bars using the parallel axis theorem.

$$J_1 = J_2 = (1/3)m_{mot}(3r_{mot}^2 + h_{mot}^2) + \dots$$
$$\dots + 4m_{mot}l^2 + (1/12)m_{hub}(l_{hub}^2 + l_{hub}^2)$$
$$J_3 = 2m_{mot}r_{mot}^2 + 4m_{mot}l^2 + \dots$$
$$\dots + (1/12)m_{hub}(l_{hub}^2 + l_{hub}^2)$$

C is the scale factor momentum - force. The input u_1 represents the impulse in the body along the z-axis, u_2 and u_3 are the angular momentum of the x-axis and the y-axis and u_4 is the momentum around the z-axis.

Therefore, the equations of motion take the following form:

$$\ddot{x} = u_1(\cos\phi\sin\theta\cos\psi + \sin\phi\sin\psi) \quad 39a$$

$$\ddot{y} = u_1(\sin\phi\sin\theta\cos\psi + \cos\phi\sin\psi) \quad 39b$$

$$\ddot{z} = u_1(\cos\theta\cos\psi) - g \quad 39c$$

$$\ddot{\theta} = u_2 l \quad 40a$$

$$\ddot{\psi} = u_3 l \quad 40b$$

$$\ddot{\phi} = u_4 \quad 40c$$

2.3. Real Helicopter

The stabilizer bar is a rotating component mounted on the same axis of the main rotor, whose function is to help the altitude control of the helicopter. This component is needed in helicopter small models (Fig. 9) due to the scale effects that makes them more agile compared to their equivalent real models.

Fig. 9. Real helicopter (small) model – *Raptor 30*.

The main rotor, besides being responsible for the lift of the helicopter, is also the main element in the control of the vehicle. The pilot can control the angle of attack of the blades in two different ways:

- Through the collective control

- Through the cyclical control

The collective control affects the angle of attack of the blades throughout the cycle, which is the primary mechanism to control the helicopter lifting.

The cyclic control pushes one side of the swash plate assembly upward or downward. This has the effect of changing the pitch of the blades unevenly depending on where they are in the rotation. The result of the cyclic control is that the rotor's wings have a greater angle of attack (and therefore more lift) on one side of the helicopter and a lesser angle of attack (and less lift) on the opposite side. The unbalanced lift causes the helicopter to tip and move laterally.

The dynamic behavior of the helicopter is derived from the six equations of the rigid body. These equations express the individual linear and angular acceleration as well as the sum of the individual influences of the coriolis accelerations, gravitational and aerodynamic effects.

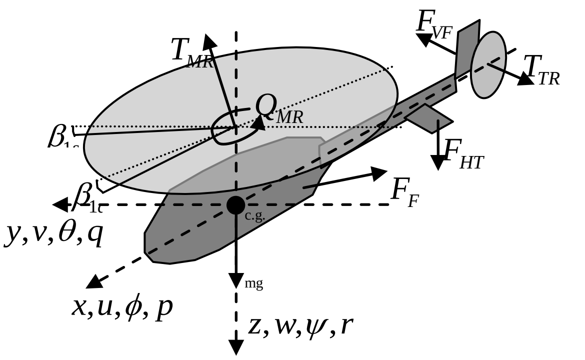

Fig. 10. Forces in the Real Helicopter.

$$\dot{u} = vr - wq - g\sin(\theta) + (X_{mr} + X_{fus})/m \quad (41a)$$

$$\dot{v} = wp - ur - g\sin(\phi)\cos(\theta) + \ldots$$
$$\ldots + (Y_{mr} + Y_{fus} + Y_{tr} + Y_{vf})/m \quad (41b)$$

$$\dot{w} = uq - vp - g\cos(\phi)\cos(\theta) + (Z_{mr} + Z_{fus} + Z_{ht})/m \quad (41c)$$

$$\dot{p} = qr(I_{yy} - I_{zz})/I_{xx} + (L_{mr} + L_{vf} + L_{tr})/I_{xx} \quad (42a)$$

$$\dot{q} = pr(I_{zz} - I_{xx})/I_{yy} + (M_{mr} + M_{ht})/I_{yy} \quad (42b)$$

$$\dot{r} = pq(I_{xx} - I_{yy})/I_{zz} + (-Q_e + N_{vf} + N_{tr})/I_{zz} \quad (42c)$$

Here, the forces and moments working on the helicopter are organized by components. The Z_{mr} represents the forces and the moments of the main rotor; L_{tr} the tail rotor; Z_{fus} the fuselage; L_{vf} the wing's vertical tail; and M_{ht} the horizontal stabilizer. Q_e is the torque produced by the engine to compensate the aerodynamic torque of the blades. (u, v, w) are the linear velocities of the vehicle in the local coordinates system. (p, q, r) are the angular velocities.

3. SIMULATION PLATFORMS

In the last two decades robotics became a common subject in courses of electrical, computer, control and mechanical engineering. Progress in scientific research and developments on industrial applications lead to the appearance of educational programs on robotics, covering a wide range of aspects such as kinematics and dynamics, control, programming, sensors, artificial intelligence, simulation and mechanical design. Nevertheless, courses on robotics require laboratories having sophisticated equipment, which pose problems of funding and maintenance.

The development of simulation platforms became an important ally of science, and today it is spread in the most varied sectors.

The computer programs emphasize capabilities such as the 3D graphical simulation and the programming language giving some importance to mathematical aspects of modeling and control [16].

However, undergraduate students with no prior experience may feel difficulties in getting into the robotics experiments before overcoming the symbolic packages procedures and commands. This state of affairs motivated the development of a computer program highlighting the fundamentals of robot mechanics and control.

The simulation platforms were developed in *MatLab* and *Simulink* for high numerical computation and performance visualizations. It allows to efficiently implement and solve mathematical problems faster than other languages such as *C*, *BASIC*, *PASCAL* or *FORTRAN*.

The educational packages were designed to take full advantage of the Windows environment. All the commands and the required parameters are entered through pull-down menus and dialog boxes. The software is intended to be self-explanatory to the extent possible to encourage students exploring the program. For the same purpose, help menus are available throughout the different windows. Several dialog boxes include figures to clarify context-dependent definitions.

3.1. TRMS Sim

The *TRMS Sim* (Fig. 11) is the simulator of the real laboratory platform using the mathematical formulation and modeling presented. The animation was developed in a *script* using the direct kinematics.

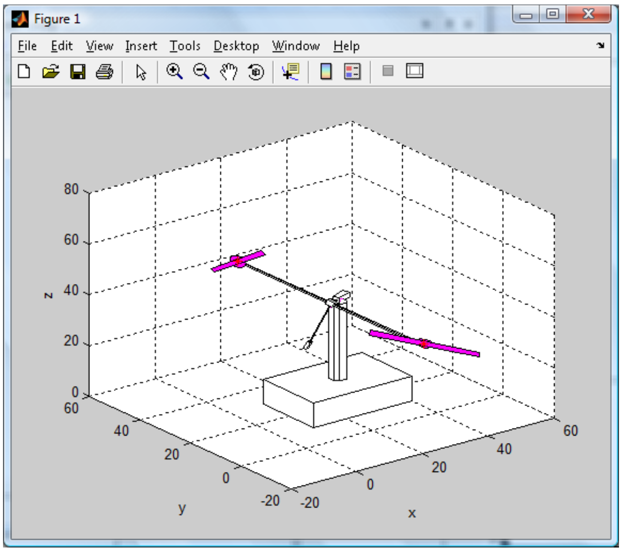

Fig. 11. Educational Package *TRMS Sim*.

The *Simulink* implementation generates 6 files (*alfav*, *alfah*, *wv*, *wh*, *Uv*, *Uh*) with the simulation results, which can then be inserted in the animation.

3.2. Quad-Rotor Sim

The *Quad-Rotor Sim* (Fig. 12) has a *VRML* (Virtual Reality Modeling Language) animation in order to visualize the animation synchronized with the data generation rate of *Simulink*. As iteration algorithm it was used the *ode4* with fixed step and a sampling rate of 0.001 seconds.

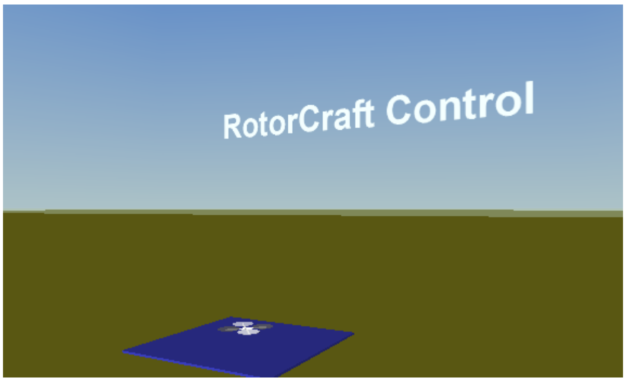

Fig. 12. Educational Package *Quad-Rotor Sim*.

It is possible to control the rotorcraft through an interface that inserts destination points defining a path (Fig. 13).

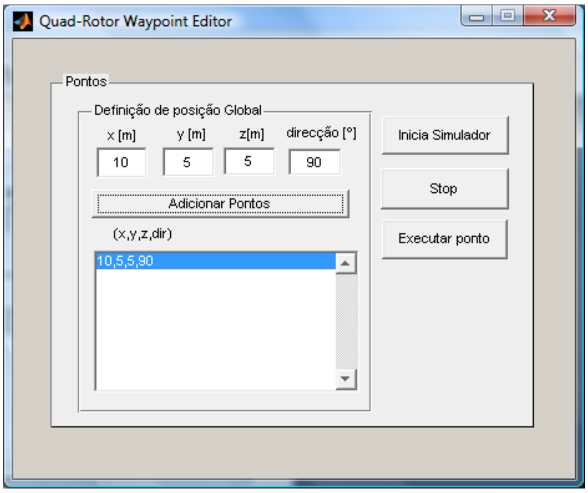

Fig. 13. Inserting destination points.

It is also possible to visualize the constant adjustments of the drivers in order to maintain the stability of the Quad-Rotor in 3D (Fig. 14).

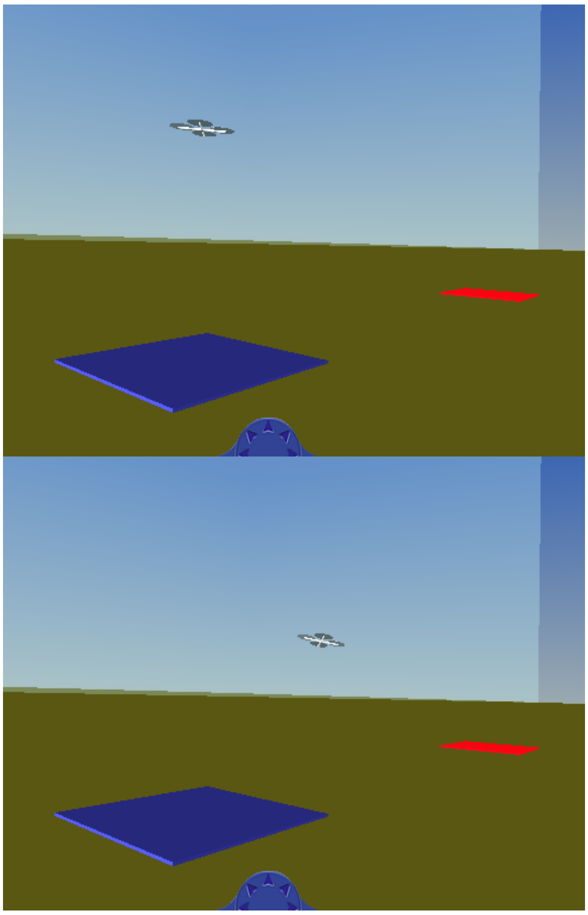

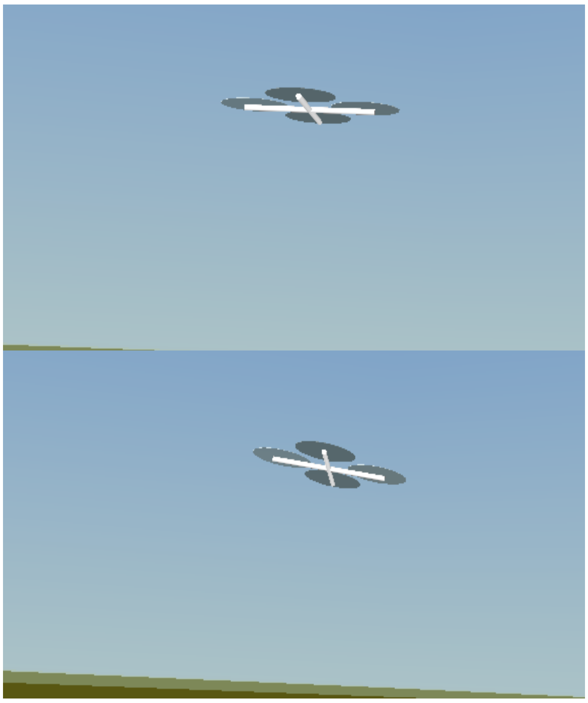

Fig. 14. Sequence of images of the *Quad-Rotor Sim* in action.

3.3. Helicopter Sim

The flight simulator *Helicopter Sim* (Fig. 15) allows the control with a joystick with a 3D animation in *VRML*. It was used the *ode45*, a variable step interaction algorithm with a sampling time of 0.01 seconds in order to obtain an acceptable animation performance.

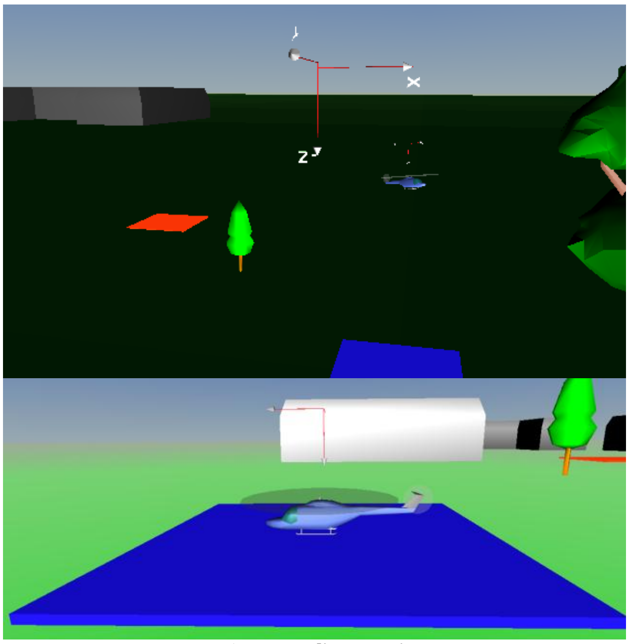

Fig. 15. *Helicopter Sim*.

4. CONCLUSION

In this paper we have proposed the design of an accurate software simulation and implementation for multiple flight platforms that includes all major components involved: aerodynamics, kinematics and external environment.

The functionalities presented in this work are implemented on the simulator. The simulation time greatly depends on the initial gains limits, the disturbances applied and the fitness function used.

The design methodology and implementation can be deemed successful in this project. By obtaining a balance between physical modeling and the objective of animation, a strong advance in the system sophistication has been achieved.

REFERENCES

[1] J. Coelho, R. Neto, D. Afonso, C. Lebres, N. M. Fonseca Ferreira and J. A. Tenreiro Machado. “Application of Fractional Algorithms in the Control of a Twin Rotor Multiple Input-Multiple Output System”. 6th EUROMECH, Conference ENOC 2008, June 30 — July 4, Saint Petersburg, Russia, 2008.

[2] J. Coelho, R. Neto, V. Santos, C. Lebres, N. M. Fonseca Ferreira and J. A. Tenreiro Machado. “Application of Fractional Algorithms in Control of a Quad Rotor Flight”. Symposium on Computational Techniques for Engineering Sciences, at Institute of Engineering of Porto, Portugal, July 21-26, 2008.

[3] J. Coelho, R. Neto, D. Afonso, C. Lebres, N. M. Fonseca Ferreira, E. J. Solteiro Pires, J. A. Tenreiro Machado, “Helicopter System Modelling and Control With Matlab”, 2nd International Conference on Electrical Engineering- CEE’07, 26-28 November, Coimbra - Portugal, 2007.

[4] Micael S. Couceiro, Carlos M. Figueiredo, N M Fonseca Ferreira and J.A. Tenreiro Machado. “Simulation of a robotic bird”. Fractional Differentiation and its Applications. Ankara, Turkey, 05 –07 November, 2008.

[5] Micael S. Couceiro, Carlos M. Figueiredo, N. M. Fonseca Ferreira and J. A. Tenreiro Machado. “Analysis and Control of a Dragonfly-Inspired Robot”. International Symposium on Computational Intelligence for Engineering Systems, November 18 – 19, Porto, 2009.

[6] L. Schenato, X. Deng, W.C. Wu, S. Sastry. “Virtual Insect Flight Simulator (VIFS): A Software Testbed for Insect Flight”. IEEE Int. Conf. Robotics and Automation, Seoul, Korea, May 2001.

[7] Z. Jane Wang. “Dissecting Insect Flight”. Annu. Rev. Fluid Mech, 183-210, 2005.

[8] Micael S. Couceiro, Carlos M. Figueiredo, N. M. Fonseca Ferreira, J. A. Tenreiro Machado “Biological inspired flying robot”, Proceedings of IDETC/CIE 2009 ASME 2009 International Design Engineering Technical Conferences & Computers and Information

in Engineering Conference August 30 - September 2, San Diego, 2009.

[9] Bar-Cohen Y., C. Breazeal. “Biologically-Inspired Intelligente Robots”. SPIE Press, Vol. PM122, May 2003.

[10] Micael S. Couceiro, Carlos M. Figueiredo, N. M. Fonseca Ferreira, J. A. Tenreiro Machado “The Dynamic Modeling of a Bird Robot”, 9th Conference on Autonomous Robot Systems and Competitions, Robotica 2009, Castelo Branco, Portugal, 07 Maio, 2009.

[11] J. Gordon Leishman. “Principles of Helicopter Aerodynamics”. Second Edition, Cambridge University Press, 2000.

[12] Martin D. Maisel, Demo J. Giulianetti and Daniel C. Dugan. “The History of the XV-15 Tilt Rotor Research Aircraft From Concept to Flight”. National Aeronautics and Space Administration Office of Policy and Plans NASA History Division Washington, D.C., 2000.

[13] Etkin B, Reid LD. “Dynamics of Flight: Stability and Control – 3rd Edition”. ISBN: 978-0-471-03418-6, 400 pages, November 1995.

[14] Stevens BL, Lewis FL. “Aircraft Control and Simulation – 2nd Edition”. ISBN: 978-0-471-37145-8, 680 pages, October 2003.

[15] M. López Martínez. F.R. Rubio. Approximate Feedback Linearization of a Laboratory Helicopter, Sixth Portuguese Conference on Automatic Control. pp.43-45, Faro, Portugal, 2004.

[16] N. M. Fonseca Ferreira, J. Machado, “RobLib: An educational program for analysis of robots”, Proceedings of Controlo 2000, 4th Portuguese Conference on Automatic Control, pg. 406-411 4-6 Oct, Guimaraes – Portugal, 2000.